
Cause-Effect Deep Information Bottleneck For Incomplete Covariates

Sonali Parbhoo*, Mario Wieser* and Volker Roth

Department of Mathematics and Computer Science, University of Basel, Switzerland
{sonali.parbhoo, mario.wieser, volker.roth}@unibas.ch

Abstract

Estimating the causal effects of an intervention in the presence of confounding is a frequently occurring problem in applications such as medicine. The task is challenging since there may be multiple confounding factors, some of which may be missing, and inferences must be made from high-dimensional, noisy measurements. In this paper, we propose a decision-theoretic approach to estimate the causal effects of interventions where a subset of the covariates is unavailable for some patients during testing. Our approach uses the information bottleneck principle to perform a discrete, low-dimensional sufficient reduction of the covariate data to estimate a distribution over confounders. In doing so, we can estimate the causal effect of an intervention where only partial covariate information is available. Our results on a causal inference benchmark and a real application for treating sepsis show that our method achieves state-of-the-art performance, without sacrificing interpretability.

1 Introduction

Understanding the causal effects of an intervention is a key question in many applications, from personalised medicine to marketing (e.g. Sun et al. (2015); Wager and Athey (2017); Alaa and van der Schaar (2017)). Predicting the causal outcome in these situations typically involves dealing with high-dimensional observational data that is frequently subject to the effects of

confounding, where the actions in the data are dependent on variables that may also indirectly influence the outcome.

In general, we distinguish between measured and hidden confounding: When confounders are directly measured, they may be accounted for using techniques that correct for their effects, such as propensity reweighting (IPS) or covariate shift (Hernán and Robins, 2006; Rosenbaum and Rubin, 1984). In contrast, to account for hidden confounding, proxy variables may be used as noisy representatives of latent confounders (Greenland and Lash, 2008; Pearl, 2012; Kuroki and Pearl, 2014; Louizos et al., 2017). While each of these approaches has its merits, the former and the latter approaches can only be applied when covariate data is completely measured. This assumption is not feasible in a large number of settings such as medicine. For example, doctors are interested in identifying treatments that improve patient outcomes, and have to base decisions on hundreds of potentially confounding variables such as age and genetic factors. Here, a doctor may readily have access to many routine measurements such as blood count data for all patients, but may only have genetic information for some patients. Inferring the causal effects of a treatment in such a setting requires learning a joint distribution over covariates and confounders of patients whose data is completely observable, while simultaneously transferring this knowledge to patients whose data is missing. In low-dimensional discrete settings, performing such a knowledge transfer is relatively straightforward as one can average over covariates and directly use this information to make inference about cases where covariates are missing. However, in high-dimensional settings this is not achievable in practice since we have to integrate over all missing covariates.

In this paper, we propose addressing the problem of performing causal inference with partial covariate information from an decision-theoretic point of view. We emphasise that our approach can be generalised to both hidden and measured confounders. Specifically,

*These authors contributed equally.
Preprint. Work in progress.

we assume that a fixed set of measurements is unavailable for a subset of the data (or patients) at test time. The key idea is to use the Information Bottleneck (IB) criterion (Tishby et al., 2000; Alemi et al., 2016) to perform a sufficient reduction of the covariate and recover a distribution of the confounding information. In particular, the IB enables us to build a discrete reference class over patients whose covariate data is complete, to which we can map patients with incomplete data and estimate treatment effects on the basis of such a mapping.

Our contributions may thus be summarised as follows: We learn a discrete, low-dimensional, interpretable latent space representation of confounding information. We use the discrete, low-dimensional representation to estimate the causal effect for data with missing covariates at test time. This representation allows us to learn equivalence classes among patients such that the specific treatment effect of a patient can be approximated by the specific treatment effect of the subgroups. Finally, we demonstrate that our method outperforms existing approaches across established causal inference benchmarks and a real world application for treating sepsis.

2 Preliminaries and Related Work

Potential Outcomes and Counterfactual Reasoning Counterfactual reasoning (CR) has drawn large attention, particularly in the medical community. Counterfactual models are essentially rooted in causal inference and may be used to determine the causal effects of an intervention. These models are formalised in terms of *potential outcomes* (Splawa-Neyman, 1923, 1990; Rubin, 1978). Assume we have two choices of taking a treatment t , and not taking a treatment (control) c . Let Y_t denote the outcomes under t and Y_c denote outcomes under the control c . The counterfactual approach assumes that there is a pre-existing joint distribution $P(Y_t, Y_c)$ over outcomes. This joint distribution is hidden since t and c cannot be applied simultaneously. Applying an action t thus only reveals Y_t , but not Y_c . In this setting, computing the effect of an intervention involves computing the difference between when an intervention is made and when no treatment is applied (Pearl, 2009; Morgan and Winship, 2015). We would subsequently choose to treat with t if,

$$\mathbb{E}[L(Y_t)] \leq \mathbb{E}[L(Y_c)] \quad (1)$$

for loss L over Y_t and Y_c respectively. Potential outcomes are typically applied to cross-sectional data (Schulam and Saria, 2017b,a) and sequential time settings. Notable examples of models for counterfactual

reasoning include Johansson et al. (2016) and Bottou et al. (2013). Specifically, Johansson et al. (2016) propose a neural network architecture called TARnet to estimate the effects of interventions. Similarly, Gaussian Process CR (GPCR) models are proposed in Schulam and Saria (2017b,a) and further extended to the multitask setting in Alaa and van der Schaar (2017). Off-policy evaluation methods in reinforcement learning (RL) offer another perspective for reasoning about counterfactuals, and have been extensively explored to estimate the outcomes of a particular policy or series of treatments based on retrospective observational data (see for example Dudík et al. (2011), Thomas and Brunskill (2016), Jiang and Li (2016)).

Importantly, none of these approaches enable estimating treatment effects in the presence of confounding and partial covariate information. We emphasise that using the IB principle to perform causal inference in these settings is (to our knowledge) novel.

Decision-Theoretic View of Causal Inference

The decision theoretic approach to causal inference focuses on studying the *effects of causes* rather than the causes of effects (Dawid, 2007). Here, the key question is *what is the effect of the causal action on the outcome?* The outcome may be modelled as a random variable Y for which we can set up a decision problem. That is, at each point, the value of Y is dependent on whether t or c is selected. The decision-theoretic view of causal inference considers the distributions of outcomes given the treatment or control, P_t and P_c and explicitly computes an expected loss of Y with respect to each action choice. Finally, the choice to treat with t is made using Bayesian decision theory if,

$$\mathbb{E}_{Y \sim P_t}[L(Y)] \leq \mathbb{E}_{Y \sim P_c}[L(Y)]. \quad (2)$$

Thus in this setting, causal inference involves comparing the expected losses over the hypothetical distributions P_t and P_c for outcome Y .

Information Bottleneck The IB principle (Tishby et al., 2000) describes an information theoretic approach which is used to compress a random variable X with respect to a second random variable Y . The compression of X is described by another random variable Z . Achieving an optimal compression requires solving the following problem,

$$\min_{p(z|x)} I(X; Z) - \lambda I(Z; Y), \quad (3)$$

under the assumption that Y and Z are conditionally independent given X . Here, I represents the mutual information between two random variables and λ controls the degree of compression. In its classical form, the IB principle is defined only for discrete random

variables. However, in recent years multiple IB relaxations for Gaussian (Chechik et al., 2005) and meta-Gaussian variables (Rey and Roth, 2012) have been proposed.

Deep Latent Variable Models Deep latent variable models have recently received remarkable attention and been applied to a variety of problems. Among these, variational autoencoders (VAEs) employ the reparameterisation trick introduced in Kingma and Welling (2013); Rezende et al. (2014) to infer a variational approximation over the posterior distribution of the latent space $p(z|x)$. Important work in this direction include Kingma et al. (2014) and Jang et al. (2017). Most closely related to the work we present here, is the application of VAEs in a healthcare setting by Louizos et al. (2017). Here, the authors introduce a Cause-Effect VAE (CEVAE) to estimate the causal effect of an intervention in the presence of noisy proxies.

Despite their differences, it has been shown that there are several close connections between the VAE framework and the IB principle. Alemi et al. (2016) introduce the Deep Information Bottleneck (DIB). This is essentially a VAE where X is replaced by Y in the decoder. In contrast, the approach in this paper considers the IB principle to perform *causal inference* in scenarios where only *partial covariate data* is available at test time.

3 Method

In this section, we present an approach based on the IB principle for estimating the causal effects of an intervention with incomplete covariate information. We refer to this model as CEIB. In recent years, there has been a growing interest in the connections between the IB principle and deep neural networks (Tishby and Zaslavsky, 2015; Alemi et al., 2016; Wieczorek et al., 2018). Here, we use the non-linear expressiveness of neural networks with the IB principle to recover a low-dimensional interpretable representation for approximating the causal effects of an intervention more effectively. In Figure 1, we illustrate an overview of the possible configurations for performing causal inference and present our model in the context of existing work. The corresponding causal graphs for Cases I and II are shown in Figure 2. The major difference between I and II is the reversal of the arrow between Z and X , and the fact that in Case II confounders are not measured, but indirectly observed via noisy proxies.

In this paper, we interpret our model from the decision-theoretic view of causal inference presented in Section 2. Like other approaches in the decision-

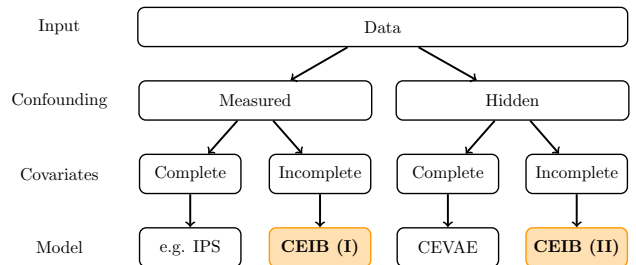


Figure 1: Overview of causal inference with confounding effects and missing covariates. In this paper, we address Cases I and II, thus accounting for incomplete covariate information when confounding is measured and hidden respectively.

theoretic setting, our goal is to estimate the *Average Causal Effect (ACE)* of T on Y . If we assume $F_T = 0$ or $F_T = 1$ define the interventional regimes, and $F_T = \emptyset$ the observational regime, the ACE is given by,

$$ACE := \mathbb{E}[Y, F_T = 1] - \mathbb{E}[Y, F_T = 0]. \quad (4)$$

Evidently, the ACE in Equation 4 is defined in terms of the interventional regime however, in practice we can only collect data on the basis of the observational regime, $F_T = \emptyset$. The observational counterpart of the ACE may formally be defined as:

$$ACE := \mathbb{E}[Y | T = 1, F_T = \emptyset] - \mathbb{E}[Y | T = 0, F_T = \emptyset]. \quad (5)$$

In general, the ACE and observational ACE are not equal as long as we assume ignorable treatment assignments. Dawid (2007) show that the ACE and observational ACE are equivalent under the conditional independence assumption $Y \perp\!\!\!\perp F_T | T$. This assumption expresses that the distribution of $Y | T$ is the same in the interventional and observational regimes. It can also be extended to account for the notion of confounding. Here, the treatment assignment F_T may be ignored when estimating Y , provided a sufficient covariate Z and T . Formally, Z is a sufficient covariate for the effect of T on outcome Y if $Z \perp\!\!\!\perp F_T$ and $Y \perp\!\!\!\perp F_T | (Z, T)$. It can also be shown via Pearl’s backdoor criterion (Pearl, 2009) that the ACE may be defined in terms of the Specific Causal Effect (SCE),

$$ACE := \mathbb{E}[SCE(Z, F_T = \emptyset)] \quad (6)$$

where

$$SCE(X) := \mathbb{E}[Y | Z, T = 1, F_T = \emptyset] - \mathbb{E}[Y | Z, T = 0, F_T = \emptyset]. \quad (7)$$



Figure 2: Influence diagrams of the two cases considered in this paper. Red and green circles correspond to observed and latent random variables respectively, while blue rectangles represent interventions. In Case I, we identify a low-dimensional representation Z of *measured* covariates X to estimate the effects of an intervention on outcome Y . In Case II, the arrow between X and Z is *reversed* and confounders are indirectly measured via proxy variables, indicated by an orange circle here. We identify a low-dimensional representation Z and use this to explicitly estimate X as well as Y . In both cases, representation Z is used to make inferences for a subset of patients where only partial covariate information is available.

In our paper, we consider the decision-theoretic approach of Dawid (2007) to estimate the causal effect where we have both hidden and measured confounding with incomplete covariates. This involves computing the ACE. Importantly, estimating the ACE only requires computing a distribution $Y|Z, T$ in Figure 2. In what follows, we use the IB to learn a sufficient covariate that allows us to approximate this distribution.

Case I: Measured Confounding This case occurs when we have a high-dimensional observational data set where all the relevant confounding variables are measured, but where a fixed set of covariates is only available for some subset of the data at test time. We propose modelling the task using a cause-effect IB with the architecture proposed in Figure 3. The IB approach allows us to learn a low-dimensional interpretable compression of the relevant information during training, which we can use to make causal inferences where data is incomplete at test time. Let X_1 and X_2 be our covariate sets (both available at training). We adapt the IB for learning the outcome of a therapy when partial covariate information is available for X_2 at test time. To do so, we consider the following parametric form,

$$\max_{\phi, \theta, \psi, \eta} -I_\phi(V_1; X_1) - I_\eta(V_2; X_2) + \lambda I_{\phi, \theta, \psi, \eta}(Z; (Y, T)), \quad (8)$$

where V_1 and V_2 are low-dimensional discrete representations of the covariate data, $Z = (V_1, V_2)$ is a concatenation of V_1 and V_2 and I represents the mutual information parameterised by networks ϕ , ψ , θ and η respectively. We assume a parametric form of the conditionals $q_\phi(v_1|x)$, $q_\eta(v_2|x)$, $p_\theta(y|t, z)$, $p_\psi(t|z)$, as well as Markov chain $Z - X - T - Y$. The three terms in

Equation 8 have the following forms:

$$\begin{aligned} I_\phi(V_1; X_1) &= D_{KL}(q_\phi(v_1|x_1)p(x_1)||p(v_1)p(x_1)) \\ &= \mathbb{E}_{p(x_1)} D_{KL}(q_\phi(v_1|x_1)||p(v_1)) \end{aligned} \quad (9)$$

$$\begin{aligned} I_\eta(V_2; X_2) &= D_{KL}(q_\eta(v_2|x_2)p(x_2)||p(v_2)p(x_2)) \\ &= \mathbb{E}_{p(x_2)} D_{KL}(q_\eta(v_2|x_2)||p(v_2)) \end{aligned} \quad (10)$$

$$\begin{aligned} I_{\phi, \theta, \psi, \eta}(Z; (Y, T)) &= \mathbb{E}_{p(x, y, t)} \mathbb{E}_{p_{\phi, \eta}(z|x)} \log p_\theta(y|t, z) \\ &\quad + \log p_\psi(t|z) + h(y), \end{aligned} \quad (11)$$

as a result of the Markov assumption in the IB model. Here $h(y) = -\mathbb{E}_{p(y)} \log p(y)$ is the entropy of y . For the decoder model, we use an architecture similar to the TARnet (Johansson et al., 2016), where we replace conditioning on high-dimensional covariates X with conditioning on latent Z . We can thus express the conditionals as,

$$\begin{aligned} p_\psi(t|z) &= \text{Bern}(\sigma(f_1(z))) \\ p_\theta(y|t, z) &= \mathcal{N}(\mu = \hat{\mu}, \sigma^2 = \hat{\sigma}), \end{aligned} \quad (12)$$

with logistic function $\sigma(\cdot)$, and outcome Y given by a Gaussian distribution parameterised with a TARnet with $\hat{\mu} = tf_2(z) + (1-t)f_3(z)$. Note that the terms f_k correspond to neural networks. While distribution $p(t|z)$ is included to ensure the joint distribution over treatments, outcomes and covariates is identifiable, in practice, our goal is to approximate the effects of a given T on Y . Hence, we train our model in teacher forcing fashion by using the true T s from data and fix the T s at test time. Since V_1 and V_2 are discrete latent representations of the covariate information, we make use of the Gumbel softmax reparameterisation trick (Jang et al., 2017) to draw samples Z from a categorical distribution with probabilities π .

Case II: Hidden Confounding This case is analogous to the work of Louizos et al. (2017), where the authors proposed a variational autoencoder approach to deal with hidden confounding in the context of proxy variables. Louizos et al. (2017) assumed a VAE architecture where they explicitly include a network for estimating $p(x|z)$ in the decoder model. This approach, however, requires the use of two auxiliary networks for predicting $p(y|t, z)$ and $p(t|z)$ for out-of-sample cases. We instead treat proxies as measured confounders and propose using Case I to estimate the causal effect here. Using Case I is permissible since both DAGs in Figure 2 are Markov equivalent, and the causal direction between X and Z can only be determined by additional assumptions on the causal graph. However, assuming the causal structure in Figure 2b as in Louizos et al. (2017) requires the definition of a complex prior over Z . In the case of a high-dimensional X with a complex dependency structure, it is extremely difficult to define such a prior in practice. Hence, it may be more natural to treat all covariates including proxies as measured confounders like we propose in this paper. In doing so, we compress the relevant information to a sufficient covariate as described in Case I.

Once we can estimate y in both cases using the proposed model, we can compute the ACE from Equation 5. The discrete representation enables us to learn equivalence classes among patients such that we can use the SCE of the subgroups from Equations 6 and 7 to approximate the individualised treatment effect. In particular, when given a test patient with partial covariates, we can assign them to the closest equivalence class of patients with similar characteristics, and approximate the effect of treatments for them on the basis of the equivalence class.

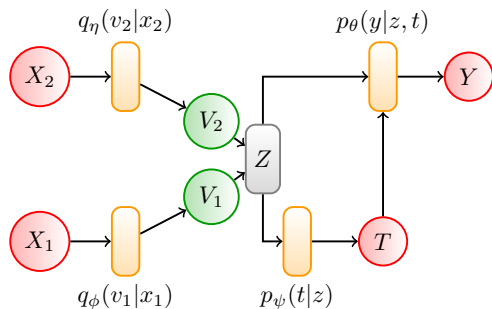


Figure 3: Graphical illustration of the CEIB. Orange rectangles represent deep networks parameterising the random variables

4 Experiments

The lack of ground truth in real world data makes evaluating causal inference algorithms a difficult problem. To overcome this issue, existing approaches typically consider a) either using synthetic or semi-synthetic data sets where the outcomes and treatment assignment are fully known or, b) using randomised control trials. We use a semi-synthetic benchmark data set from McCormick et al. (2013) that is frequently used in many causal inference studies. We also demonstrate the performance of our approach on a high-dimensional real world task for managing and treating sepsis. Our implementation uses Tensorflow (Abadi et al., 2015), and the neural architectures considered in experiments (unless otherwise stated) have 3 hidden layers. Our model is trained with the Adam optimiser (Kingma and Ba, 2014) with a learning rate of 0.001. An additional experiment using a binary twins benchmark is provided in the supplement (Almond et al., 2005).

4.1 Infant Health and Development Program

The Infant Health and Development Program (IHDP) (McCormick et al., 2013; Hill, 2011) is a randomised control experiment assessing the impact of educational intervention on outcomes of pre-mature, low birth weight infants born in 1984-1985. Measurements from children and their mother were collected for studying the effects of childcare and home visits from a trained specialist on test scores. Briefly, the study contains information about the children and their mothers/caregivers. Data on the children include treatment group, sex, birth weight, health indices. Information about the mothers includes maternal age, mother’s race as well as educational achievement. Hill (2011) extract features and treatment assignments from the real-world clinical trial, and introduce selection bias to the data artificially by removing a non-random portion of the treatment group, in particular children with non-white mothers. In total, the data set consists of 747 subjects (139 treated, 608 control), each represented by 25 covariates measuring properties of the child and their mother. The data set is divided into 60/20/20% into training/validation/testing sets.

For our experiment, we compare the performance of the proposed approach for predicting the ACE against several existing baselines. Descriptions about these baselines can be found in the supplement. We train our model with $k = 4$, $d = 3$ -dimensional Gaussian mixture components, although our method can be applied without loss of generality to any number of dimensions. To assess the ability to estimate treatment effects on the basis of partial information, we artificially exclude

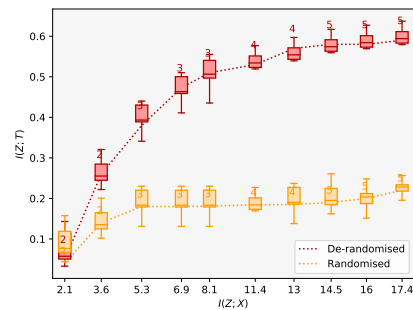
Method	$\epsilon_{ACE}^{within-s}$	$\epsilon_{ACE}^{out-of-s}$
OLS-1	.73 ± .04	.94 ± .06
OLS-2	.14 ± .01	.31 ± .02
KNN	.14 ± .01	.79 ± .05
BLR	.72 ± .04	.93 ± .05
TARnet	.26 ± .01	.28 ± .01
BNN	.37 ± .03	.42 ± .03
RF	.73 ± .05	.96 ± .06
CEVAE	.34 ± .01	.46 ± .02
CFRW	.25 ± .01	.27 ± .01
CEIB	.15 ± .02	.23 ± .01

Table 1: Within-sample and out-of-sample mean and standard errors for the metrics across models on the IHDP data set. A smaller value indicates better performance. Bold values indicate the method with the best performance.

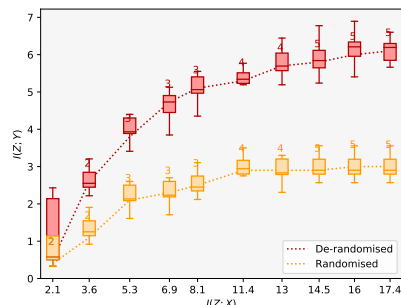
three covariates at test time. These are covariates that exhibit a moderate correlation to the hidden confounder ethnicity. The results are shown in Table 1. Overall, our approach exhibits good performance for both in-sample and out-of-sample predictions, while simultaneously accounting for partial covariate information.

To assess the interpretability of the proposed approach and the ability to account for hidden confounding, we perform an analysis on the latent space of our model. First, we plot two information curves illustrating the number of latent dimensions required to reconstruct the output for the terms $I(Z;Y)$ and $I(Z;T)$ respectively. These results are shown in Figure 4a and Figure 4b. In particular, we perform this analysis when the data set of subjects is both de-randomised and randomised (i.e. when we do not introduce selection bias into the data set). Comparing the information curves in Figure 4a confirms that when we do not de-randomise the data, the information content in the treatment $I(Z;T)$ tends to be closer to 0, whereas the opposite is true when the data is de-randomised. The information curves in Figure 4b additionally demonstrate our model’s ability to account for indirect effects of confounding when predicting the overall outcomes: when data is de-randomised, we are able to reconstruct treatment outcomes more accurately. Overall, the results from Figures 4a and 4b highlight that there is indeed a hidden confounding effect that we can account for using the proposed approach.

Next, we perform an analysis of the discretised latent space by comparing the proportions of ethnic groups of test subjects in each cluster from the Gaussian mixture to see if we can recover the hidden confounding effect. These results are shown in Figure 5 where we plot a hard assignment of test subjects to clusters on



(a)



(b)

Figure 4: (a) Information curves for $I(Z;T)$ and (b) $I(Z;Y)$ with de-randomised and randomised data respectively. When the data is randomised, the value of $I(Z;T)$ is close to zero. The differences between the curves illustrates confounding. When data is de-randomised, we are able to estimate treatment effects more accurately by accounting for this confounding.

the basis of their ethnicity. Evidently, the clusters exhibit a clear structure with respect to the ethnic groups. In particular, Cluster 2 in Figure 5b has a significantly higher proportion of non-white members in the de-randomised setting, confirming that we are able to correctly identify the true confounding effect and account for this when making predictions. Finally, we perform similar analyses and assess the error in estimating the ACE when varying the number of mixture components in Figure 7. When the number of clusters is larger, the clusters get smaller and it becomes more difficult to reliably estimate the ACE since we average over the cluster members to account for partial covariate information at test time. Here, model selection is made by observing where the error in estimating the ACE stabilises (anywhere between 4-7 mixture components).

4.2 Sepsis Management

We illustrate the performance CEIB on the real-world task of managing and treating sepsis. Sepsis is one

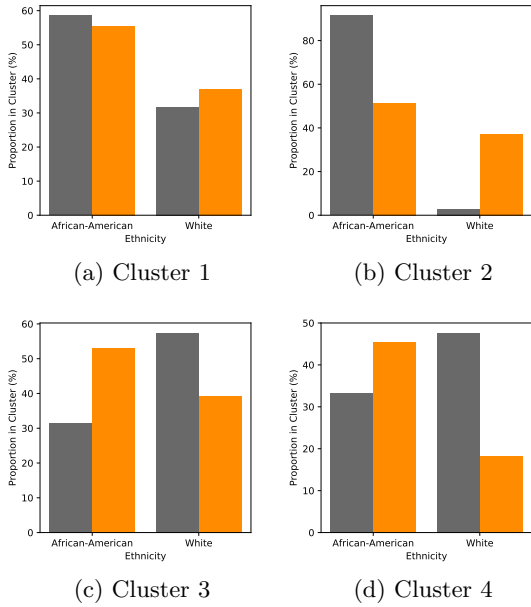


Figure 5: Illustration of the proportion of major ethnic groups within the four clusters. Grey and orange indicate de-randomised and randomised data respectively. The first cluster in (a) is a neutral cluster. The second cluster in (b) shows an enrichment of information in the African-American group. Clusters 3 and 4 in (c) and (d) respectively, show an enrichment of information in the White group. Overall, we are able to identify the hidden confounder correctly and account for this when predicting outcomes. For better visualisation, we only report the two main clusters which include the majority of all patients.

of the leading causes of mortality within hospitals and treating septic patients is highly challenging, since outcomes vary with interventions and there are no universal treatment guidelines. For this experiment, we make use of data from the Multiparameter Intelligent Monitoring in Intensive Care (MIMIC-III) database (Johnson et al., 2016). We focus specifically on patients satisfying Sepsis-3 criteria (16 804 patients in total). For each patient, we have a 48-dimensional set of physiological parameters including demographics, lab values, vital signs and input/output events, where covariates are partially incomplete. Our outcomes y correspond to the odds of mortality, while we binarise medical interventions t according to whether or not a vasopressor is administered. The data set is divided into 60/20/20% into training/validation/testing sets. We train our model with 6, 4-dimensional Gaussian mixture components and analysed the information curves and cluster compositions respectively.

The information curves for $I(Z;T)$ and $I(Z;Y)$ are shown in Figures 6a and 6b respectively. We observe

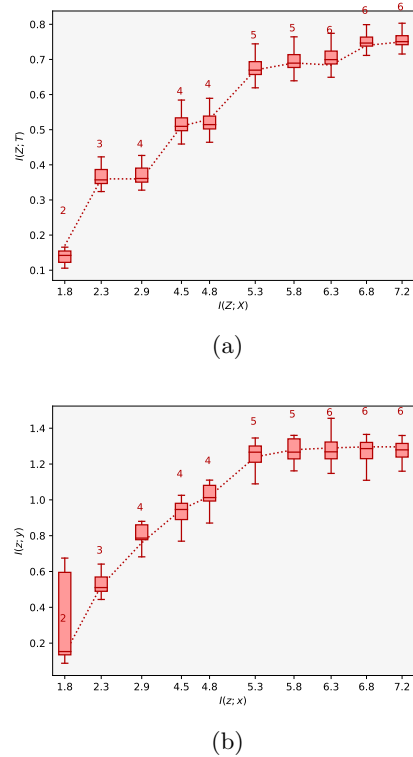


Figure 6: Subfigures (a) and (b) illustrate the information curve $I(Z;T)$ and $I(Z;Y)$ for the task of managing sepsis. We perform a sufficient reduction of the covariates to 6-dimensions and are able to approximate the ACE on the basis of this.

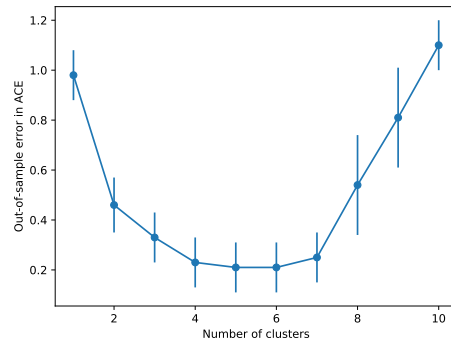


Figure 7: Out-of-sample error in ACE with a varying number of clusters.

that we can perform a sufficient reduction of the high-dimensional covariate information to between 4 and 6 dimensions while achieving high predictive accuracy of outcomes y . Since there is no ground truth available for the sepsis task, we do not have access to the true confounding variables. However, we can perform an analysis on the basis of the clusters obtained over the

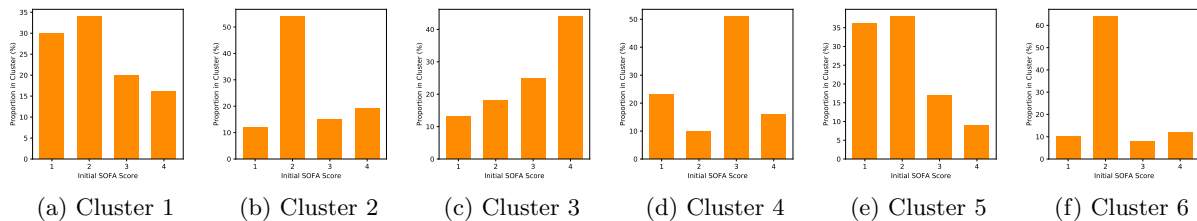


Figure 8: Proportion of initial SOFA scores in each cluster. The variation in initial SOFA scores across clusters suggests that it is a potential confounder of odds of mortality when managing and treating sepsis.

latent space. Here, we see that we can characterise the patients in each cluster according to their initial SOFA (Sequential Organ Failure Assessment) scores. SOFA scores range between 1-4 and are used to track a patient’s stay in hospital. In Figure 8, we observe clear differences in cluster composition relative to the SOFA scores. Clusters 2, 5 and 6 tend to have higher proportions of patients with lower SOFA scores, while Clusters 3 and 4 have larger proportions of patients with higher SOFA scores. This result suggests that a patient’s initial SOFA score is potentially a confounder when determining how to administer subsequent treatments and predicting their odds of in-hospital mortality. This is consistent with medical studies such as Medam et al. (2017); Studnek et al. (2012) where authors indicate that high initial SOFA scores were likely to impact on their overall chances of survival and treatments administered in hospital.

Finally, while we cannot quantify an error in estimating the ACE since we do not have access to the counterfactual outcomes, we can still compute the ACE for the sepsis management task. Here, we specifically observe a *negative* ACE value. This means that in general, treating patients with vasopressors reduces the chances of mortality in comparison to not treating patients with vasopressors. Overall, performing such analyses for tasks like Sepsis may help correct for confounding and assist in establishing potential guidelines.

5 Discussion

CEIB learns a low-dimensional, interpretable representation of latent confounding Since CEIB extracts only the information that is relevant for making predictions, it is able to learn a *low-dimensional* representation of the confounding effect and uses this to make predictions. In particular, the introduction of a discrete cluster structure in the latent space allows an easier interpretation of the confounding effect. For the IHDP experiment, we are able to learn a low-dimensional representation that is consistent with the known ethnicity confounder and ac-

count for its effects when making predictions of treatment outcomes. Similar methods such as Louizos et al. (2017) typically use a higher dimensional representation (in the order of 20 dimensions) to account for these effects and make less accurate predictions nonetheless. This is potentially a consequence of misrepresenting the true confounding effect. Modelling the task as an IB alleviates this problem. Analogously, for the sepsis task we identify a latent space of 6 dimensions when predicting odds of mortality, where clusters exhibit a distinct structure with respect to a patient’s initial SOFA score. In both tasks, the low dimensional representation enables us to accurately identify confounders without sacrificing interpretability.

CEIB enables estimating the causal effect with incomplete covariates. Unlike previous approaches, CEIB can deal with incomplete covariate data during test time by introducing a discrete latent space. Specifically, we learn equivalence classes among patients such that the approximate the effects of treatments can be computed where data is incomplete.

CEIB makes state-of-the-art predictions of the ACE that are robust against confounding Across the IHDP dataset, we see that predictions of the ACE are more accurate than existing approaches. In the IHDP case, we see reductions in the error in estimating the ACE up to 0.58 for in-sample predictions. This performance is sustained when making out-of-sample predictions we see error reductions of between 0.04 and 0.73 in comparison with existing methods. Overall, we attribute this increase in performance directly to the fact that CEIB extracts *only the information that is causally relevant for making predictions*. Proxy-based approaches such as Louizos et al. (2017) do not explicitly trade off learning meaningful representations of latent confounders and achieving accurate predictions. In contrast, we can explicitly inspect the information curves in Figure 4b and adjust compression parameter λ to uncover the true latent confounder. If we set $\lambda = 13$ in accordance to Figure 4b, we require only a 4-dimensional representation to adequately account for and uncover the true confounding

effect Z (as shown in Figure 5b). This produces more accurate predictions as a result.

6 Conclusion

We have presented a novel approach to estimate causal relationships with respect to incomplete covariates from an decision-theoretic point of view. For this purpose, we analysed the role of a sufficient covariate in the context of the IB framework to estimate the causal effect. By introducing a discrete latent space, we can estimate the causal effect if parts of the covariates are missing during test time, while accounting for both measured and hidden confounders. In contrast to previous methods, the compression parameter λ in the IB framework allows for a task-dependent adjustment of the latent dimensionality. Directions for future work include modelling structured hidden confounders as well as adopting CEIB to implicit generative models.

References

- Martín Abadi, Ashish Agarwal, Paul Barham, Eugene Brevdo, Zhifeng Chen, Craig Citro, Greg S. Corrado, Andy Davis, Jeffrey Dean, Matthieu Devin, Sanjay Ghemawat, Ian Goodfellow, Andrew Harp, Geoffrey Irving, Michael Isard, Yangqing Jia, Rafal Jozefowicz, Lukasz Kaiser, Manjunath Kudlur, Josh Levenberg, Dandelion Mané, Rajat Monga, Sherry Moore, Derek Murray, Chris Olah, Mike Schuster, Jonathon Shlens, Benoit Steiner, Ilya Sutskever, Kunal Talwar, Paul Tucker, Vincent Vanhoucke, Vijay Vasudevan, Fernanda Viégas, Oriol Vinyals, Pete Warden, Martin Wattenberg, Martin Wicke, Yuan Yu, and Xiaoqiang Zheng. TensorFlow: Large-scale machine learning on heterogeneous systems, 2015. Software available from tensorflow.org.
- Ahmed M. Alaa and Mihaela van der Schaar. Bayesian inference of individualized treatment effects using multi-task gaussian processes. *CoRR*, abs/1704.02801, 2017.
- Alexander A. Alemi, Ian Fischer, Joshua V. Dillon, and Kevin. Murphy. Deep Variational Information Bottleneck. *ArXiv e-prints*, December 2016.
- Douglas Almond, Kenneth Y Chay, and David S Lee. The costs of low birth weight. *The Quarterly Journal of Economics*, 120(3):1031–1083, 2005.
- Léon Bottou, Jonas Peters, Joaquin Quiñero-Candela, Denis X Charles, D Max Chickering, Elon Portugaly, Dipankar Ray, Patrice Simard, and Ed Snelson. Counterfactual reasoning and learning systems: The example of computational advertising. *The Journal of Machine Learning Research*, 14(1):3207–3260, 2013.
- Gal Chechik, Amir Globerson, Naftali Tishby, and Yair Weiss. Information bottleneck for gaussian variables. In *Journal of Machine Learning Research*, pages 165–188, 2005.
- Philip Dawid. Fundamentals of statistical causality. Technical report, Department of Statistical Science, University College London, 2007.
- Miroslav Dudík, John Langford, and Lihong Li. Doubly robust policy evaluation and learning. *arXiv preprint arXiv:1103.4601*, 2011.
- Sander Greenland and Timothy Lash. Bias analysis. *Modern Epidemiology*, pages 345 – 380, 2008.
- Miguel A Hernán and James M Robins. Estimating causal effects from epidemiological data. *Journal of Epidemiology & Community Health*, 60(7):578–586, 2006.
- Jennifer L. Hill. Bayesian nonparametric modeling for causal inference. *Journal of Computational and Graphical Statistics*, 20(1):217–240, 2011.
- E. Jang, S. Gu, and B. Poole. Categorical Reparameterization with Gumbel-Softmax. *International Conference on Learning Representations (ICLR)*, 2017.
- Nan Jiang and Lihong Li. Doubly robust off-policy value evaluation for reinforcement learning. In *International Conference on Machine Learning*, pages 652–661, 2016.
- Fredrik D. Johansson, Uri Shalit, and David Sontag. Learning representations for counterfactual inference. In *Proceedings of the 33rd International Conference on International Conference on Machine Learning - Volume 48, ICML’16*, pages 3020–3029. JMLR.org, 2016.
- Alistair EW Johnson, Tom J Pollard, Lu Shen, H Lehman Li-wei, Mengling Feng, Mohammad Ghassemi, Benjamin Moody, Peter Szolovits, Leo Anthony Celi, and Roger G Mark. Mimic-iii, a freely accessible critical care database. *Scientific data*, 3:160035, 2016.
- Diederik P. Kingma and Jimmy Ba. Adam: A method for stochastic optimization. abs/1412.6980, 2014.
- Diederik P Kingma and Max Welling. Auto-encoding variational bayes. *arXiv preprint arXiv:1312.6114*, 2013.
- Diederik P. Kingma, Shakir Mohamed, Danilo Jimenez Rezende, and Max Welling. Semi-supervised learning with deep generative models. In *Advances in Neural Information Processing Systems 27: Annual Conference on Neural Information Processing Systems 2014, December 8-13 2014, Montreal, Quebec, Canada*, pages 3581–3589, 2014.

- Manabu Kuroki and Judea Pearl. Measurement bias and effect restoration in causal inference. *Biometrika*, 101(2):423–437, 2014.
- Christos Louizos, Uri Shalit, Joris M Mooij, David Sontag, Richard Zemel, and Max Welling. Causal effect inference with deep latent-variable models. In I. Guyon, U. V. Luxburg, S. Bengio, H. Wallach, R. Fergus, S. Vishwanathan, and R. Garnett, editors, *Advances in Neural Information Processing Systems 30*, pages 6446–6456. Curran Associates, Inc., 2017.
- Marie C. McCormick, Jeanne Brooks-Gunn, and Stephen L. Buka. Infant health and development program, phase iv, 2001-2004 [united states]. 2013. doi: 10.3886/ICPSR23580.v2.
- Sophie Medam, Laurent Zieleskiewicz, Gary Duclos, Karine Baumstarck, Anderson Loundou, Julie Alin-grin, Emmanuelle Hammad, Coralie Vigne, François Antonini, and Marc Leone. *Medicine*, 96(50), 12 2017. doi: 10.1097/MD.0000000000009241.
- Stephen L Morgan and Christopher Winship. *Counterfactuals and causal inference*. Cambridge University Press, 2015.
- Judea Pearl. *Causality*. Cambridge university press, 2009.
- Judea Pearl. On measurement bias in causal inference. *arXiv preprint arXiv:1203.3504*, 2012.
- Mélanie Rey and Volker Roth. Meta-gaussian information bottleneck. In Peter L. Bartlett, Fernando C. N. Pereira, Christopher J. C. Burges, Lon Bot-tou, and Kilian Q. Weinberger, editors, *NIPS*, pages 1925–1933, 2012.
- Danilo Jimenez Rezende, Shakir Mohamed, and Daan Wierstra. Stochastic backpropagation and approximate inference in deep generative models. In Eric P. Xing and Tony Jebara, editors, *Proceedings of the 31st International Conference on Machine Learning*, volume 32 of *Proceedings of Machine Learning Research*, pages 1278–1286, Beijing, China, 22–24 Jun 2014. PMLR.
- Paul R Rosenbaum and Donald B Rubin. Reducing bias in observational studies using subclassification on the propensity score. *Journal of the American statistical Association*, 79(387):516–524, 1984.
- Donald B Rubin. Bayesian inference for causal effects: The role of randomization. *The Annals of statistics*, pages 34–58, 1978.
- Peter Schulam and Suchi Saria. What-if reasoning using counterfactual gaussian processes. In *Advances in Neural Information Processing Systems 30: Annual Conference on Neural Information Processing Systems 2017, 4-9 December 2017, Long Beach, CA, USA*, pages 1696–1706, 2017a.
- Peter Schulam and Suchi Saria. Reliable decision support using counterfactual models. In I. Guyon, U. V. Luxburg, S. Bengio, H. Wallach, R. Fergus, S. Vishwanathan, and R. Garnett, editors, *Advances in Neural Information Processing Systems 30*, pages 1697–1708. Curran Associates, Inc., 2017b.
- Uri Shalit, Fredrik D. Johansson, and David Sontag. Estimating individual treatment effect: generalization bounds and algorithms. In Doina Precup and Yee Whye Teh, editors, *Proceedings of the 34th International Conference on Machine Learning*, volume 70 of *Proceedings of Machine Learning Research*, pages 3076–3085, International Convention Centre, Sydney, Australia, 06–11 Aug 2017. PMLR.
- Jerzy Splawa-Neyman. Sur les applications de la théorie des probabilités aux expériences agricoles: Essai des principes. *Roczniki Nauk Rolniczych*, 10: 1–51, 1923.
- Jerzy Splawa-Neyman. On the application of probability theory to agricultural experiments. essay on principles. section 9. *Statistical Science*, 5(4):465–472, 1990.
- Jonathan R Studnek, Melanie R Artho, Craymon L Garner Jr, and Alan E Jones. The impact of emergency medical services on the ed care of severe sepsis. *The American journal of emergency medicine*, 30(1):51–56, 2012.
- Wei Sun, Pengyuan Wang, Dawei Yin, Jian Yang, and Yi Chang. Causal inference via sparse additive models with application to online advertising. In *AAAI*, pages 297–303, 2015.
- Philip Thomas and Emma Brunskill. Data-efficient off-policy policy evaluation for reinforcement learning. In *International Conference on Machine Learning*, pages 2139–2148, 2016.
- Naftali Tishby and Noga Zaslavsky. Deep learning and the information bottleneck principle. *CoRR*, abs/1503.02406, 2015.
- Naftali Tishby, Fernando C Pereira, and William Bialek. The information bottleneck method. *arXiv preprint physics/0004057*, 2000.
- Stefan Wager and Susan Athey. Estimation and inference of heterogeneous treatment effects using random forests. *Journal of the American Statistical Association*, 2017.
- Aleksander Wieczorek, Mario Wieser, Damian Murezan, and Volker Roth. Learning Sparse Latent Representations with the Deep Copula Information Bottleneck. *International Conference on Learning Representations (ICLR)*, 2018.

A Infant Health and Development Program: Baselines

For our experiments, we compare the performance of CEIB for predicting the ACE against several existing baselines as in Louizos et al. (2017): OLS-1 is a least squares regression; OLS-2 uses two separate least squares regressions to fit the treatment and control groups respectively; TARnet is a feedforward neural network respectively; TARnet is a feedforward neural network from Shalit et al. (2017); KNN is a k -nearest neighbours regression; RF is a random forest; BNN is a balancing neural network (Johansson et al., 2016); BLR is a balancing linear regression (Johansson et al., 2016), and CFRW is a counterfactual regression that using the Wasserstein distance (Shalit et al., 2017).

B Additional Experiments

B.1 Binary Treatment Outcome on Twins

Like Louizos et al. (2017), we apply CEIB to a benchmark task using the birth data of twins in the USA between 1989 and 1991 (Almond et al., 2005). Here, treatment $T = 1$ is a binary indicator of being the heavier twin at birth, while outcome Y corresponds to the mortality within a year after birth. Since mortality is rare, we consider only same sex twins with weights less than 2 kg which results in 11 984 pairs of twins. Each twin has a set of 46 covariates including information about their parents such as their level of education, race, incidence of renal disease, diabetes, smoking etc. as well as whether the birth took place in hospital or at home and the number of gestation weeks prior to birth.

To simulate an observational study, we selectively hide one of the twins. To illustrate the ability of CEIB to be applied to Case II where we treat proxy variables as measured confounders, we base the treatment assignment on a single variable which is highly correlated with the outcome: GESTAT10, the number of gestation weeks prior to birth. This has values from 0-9 that correspond to the weeks of gestation before birth i.e. birth before 20 weeks gestation, 20-27 weeks of gestation, etc. Analogous to Louizos et al. (2017) we set treatment to $t|x, z \sim \text{Bern}(\sigma(w_o^\top x + w_h(z/10 - 0.1)))$ for $w_o \sim \mathcal{N}(0, 0.1I)$, $w_h \sim \mathcal{N}(5, 0.1)$, where z is GESTAT10 and x are the 45 remaining covariates. Since CEIB can account for incomplete covariates, we artificially exclude 3 covariates from x at test time.

Like Louizos et al. (2017), proxies are created with a one-hot encoding of z , replicated 3 times and randomly flipping the 30 bits, where the flipping probability varies from 0.05 to 0.15. There may also be additional proxy variables for z in the data from the set

of variables. Our task is to predict the ACE. Specifically, we compare the performance of CEIB to CEVAE (with a varying number of hidden layers), TARnet (with varying numbers of hidden layers) and logistic regression (LR). These results are shown in Figure 9. Here too, CEIB achieves close to state-of-the-art performance on the Twins task.

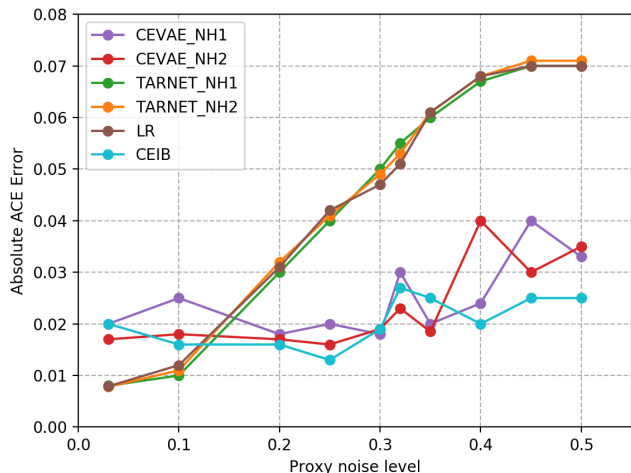


Figure 9: Absolute error in ACE estimation for Twins task. CEIB outperforms baselines over varying levels of proxy noise.